Lung Nodule Detection Based on Noise Robust Local Binary Pattern

Mohammad Hossein Shakoor

Abstract— In this paper a new method for detection of lung nodules in CT image is proposed which is robust to noise. For nodule detection, two important steps are followed: feature extraction and classification. For features extraction, some texture features are extracted based on an extended type of Local Binary Pattern (LBP). LBP is one of the most important feature extractor in texture image but one of the drawback of it, relates to noise because LBP is more sensitive to noise. The key point of the proposed LBP is robustness to noise by using uniform texture information. Support Vector Machine (SVM) is used for classification to distinct the pathological change (nodule) from other normal regions of the chest.

Index Terms— Local binary pattern, nodule detection, uniform pattern, noise robust LBP.

1 INTRODUCTION

LONG Lung cancer is the most common cause of cancer deaths in the world. In the last few years, many computer-aided detection (CAD) systems have been proposed to help radiologists to diagnose diseases such as automatic detection of lung nodules in CT scans [1]. These systems make it possible to detects diseases very faster than a specialist alone. Recent research has demonstrated the advantages of using CAD systems to help physicians in the detection [2-4] and diagnosis of lung cancer[8]. A CAD system for CT images includes three important parts: 1) preprocessing and lung segmentation, 2) features extraction part that extracts features of each sub-region of CT image by using some descriptors and 3) A classifier that divides sub-regions of CT images into normal and abnormal (nodule).

At the beginning of the algorithm some prepossessing operations must be applied on each CT image. Then lung curve should be extracted to exclude all redundant parts from each CT image.[5-9]. Also there are many features that can be used for classification. The texture features are fundamental features for image segmentation [10,11], image classification [12,13], image retrieval systems [14,15], etc. In the past 10 years, some methods based on the texture features were proposed. These methods such as the gray level difference method (GLDM), the gray level run-length method (GLRLM), and the spatial gray level dependent method (SGLDM) [16] have been widely used to extract medical image characteristics and structures that are not directly visible for observers.

There are some automatic methods for lung nodule detection. Most of these methods use segmentation before classification in lung image to extract nodules of image. Ozekes [17], used a segmentation algorithm based on rules and template matching trained with genetic algorithm (GA) which achieved 93.4% sensitivity and 0.59% false positives per exam. Ozekes et al. [18] achieved 100% sensitivity and a rate of 13.37% false genetic neural network and threshold based on fuzzy rules.

In [19], Ye et al. used a set of different features, containing intensity information, shape index, and 3D spatial location for nodule detection. Antonelli et al. [20], used fuzzy c-means, followed by a morphological analysis of the resulting structures for this purpose. The automatic detection of low-dose CT images (LDCT) was reported in [21] using information from probabilistic models created to control the evolution of a deformable model, that was able to segment the lung nodules with low average error and low standard deviation with respect to the form described by the specialist. In [22] Messay et al. combined simple image processing techniques, such as intensity thresholding and morphological operations, to segment and detect structures that were lung nodule candidates. The authors did feature selection among 245 features to determine the lung nodule candidates and used them in two classifiers: the Fisher Linear Discriminant classifier and a quadratic classifier. The method was able to detect 92.8% of the structures, which were nodule candidates. The CAD system proposed by Tan et al. [23] employed three classifiers; one of them is based on genetic algorithms and artificial neural networks, which are then, compared to results from SVM and fixed-topology neural networks. The lung nodule detection method includes filters to detect nodules and vessels, and divergence features to locate possible lung nodule candidates. Once the candidates are detected, features in a gauge system are applied to the three classifiers. The results obtained with the fixed-topology neural network had sensitivity of 87.5%, with average of four false positives per exam for nodules with diameter larger than or equal to 3 mm. Opfer et al. [24] have shown how to evaluate the performance of CAD systems using a standard dataset, which has the ground truth given by four specialists. In their analyses, the authors showed that their CAD system is able to reach detection rate of 89% of the lung nodules.

Because of some special texture of nodule of CT images, texture features are widely used for nodule detection. One of the most important descriptors that can provide feature of texture accurately is Local Binary Pattern (LBP) [25]. LBP is a powerful texture descriptor that is widely used in various applica-

• *Mohammad Hossein Shakoor, Fars Science and Research Branch, Islamic Azad University, Shiraz, Iran, E-mail: mhshakoor@gmail.com*

tions to extract some texture features. The LBP^{riu2} [26] is rotation invariant LBP by using the uniform local pattern. To further benefit from the uniform local pattern is extended LBP (ELBP) that can be used as a good measure of an image's uniformity. In most paper each segmented lung is divided into some sub-regions and for each sub-region, texture features are extracted from the co-occurrence matrix. The co-occurrence matrix is made based on ELBP and Gradient of Difference (GOD) of each point. Then the features of each sub-region are fed into Support Vector Machine
(SVM) to classify each sub-region into nodule and normal region.

This paper is organized as follows: Section 2 presents preprocessing and lung segmentation of system, Section 3 describes feature extraction method and proposed method, experimental results and conclusion are shown in sections 4 and 5, respectivly.

2 Preprocessing and Lung Segmentation

Before using nodule detection process, It is necessary to enhance CT images and remove some redundant region of images. Some types of noises are removed by median filter because this filter has high noise removing ability and low blurring effect comparison with other filters[27]. But, it is not possible to remove all of the noise. So in the proposed method a local binary pattern method is proposed that correct the effects of noise. Also images are enhanced by gamma correction. Fig.1a-1c represent original image, denoised image and enhanced image. After image enhancement, it is necessary to extract lung curve from other parts. In other images in Fig 1. A binary image is obtained by Otsu method [28] and the border of the lung region in each slice is extracted by canny edge detection method. Fig.1f-1g show that some nodules that attach to chest wall are removed.

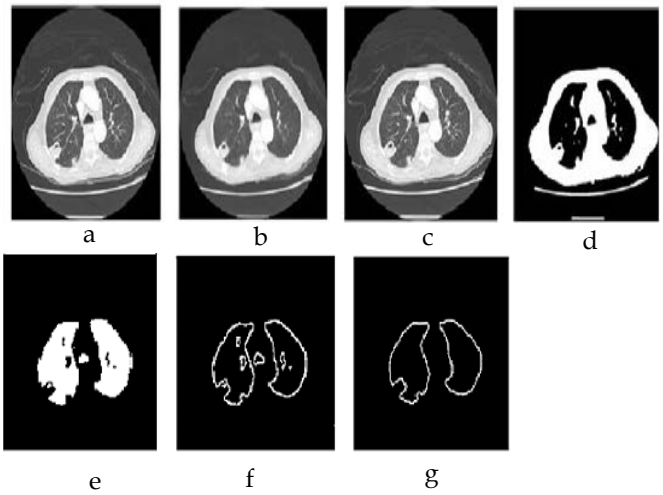

Fig. 1. Preprocessing images: a) Original image; b) Denoised image; c) Enhanced image; d) Binarized image; e) Cleaned binarized; f) Whole contours; g) Lung contour.

The lung segmentation process should consider these nodules as lung parts to segment them in nodule detection. Here, by using concavity degree of border this problem is solved. In this method the lung borders are traced in a sequence of n pixels, so they form a collection of directed closed contours and extra contours are removed based on the number of pixels in each contour. Fig.2a-2b represents results of these steps.
Concavity degree computation of each boundary pixel corresponds to boundary points by distance that are considered as two endpoints of the base line. The base line determines the type of point (convex or concave). Thus, this base line is plotted and its points that are not on the region are counted. The concavity degree defines as the ratio of the number of outside points toward the base line and the total number of the line segment points. Fig.2b shows extracted lung from the original CT image.

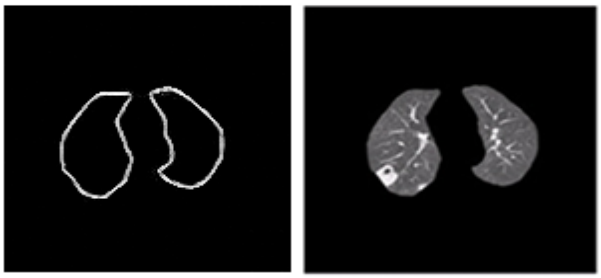

Fig. 2. Result of lung segmentation: a) Lung contour; b) Extracted lung.

3 Features Extraction and Nodule detection

In this section, nodules will be detected by classifying the pixels in segmented lungs to two classes: nodule area and normal area. Same as every classification system, this paper follows two steps: feature extraction and classification. Texture features are obtaining and SVM classifier is used for classification.

3.1 Features Extraction

After enhancement of CT images and extracted of lung curve. Then features must be extracted from these lung images. For lung CT images there are many features which can be used for classification such as shape, intensity, texture and so on. Because of the texture characteristics of nodules and pathological change of the tissues of lung, texture features are widely used for obtaining the discriminative information from CT images [29]. To extract the texture features from the lung and recognize nodule regions, each image is separated into sub-regions as Liang, Tanaka and Nakamura [30] did. Fig.3a and Fig.3b show the sub-regions of a lung image for small and large sub-region respectively. Value of d (dimension of square sub-region) must be selected properly. If it is so large, it may decrease accuracy of classification. On the other hand, using very small sub-regions increases the number of train and test data and results in high computational complexity for train and test operations. Therefore, d should be set same as the size of diameter of medium nodules. For nodule detection it is possible to use large sub-region to determine only the sub-region (location) of each nodule. All sub-regions are not used for feature extraction, because there are some only black or only white sub-regions that do not have any information. In Fig.3a and

Fig.3b these parts are white or black completely. For each sub-region, the Extended LBP values are mixed with gradient difference to make co-occurrence matrix which is used to extract some features for classification.

Nodules in the CT images have especial texture structure. In order to make distinction between nodules and the normal regions, some features are required. For this purpose, Penget proposed the uniformity estimation method (UEM) [29] based on local binary pattern (LBP), which can extract the uniformity information of brightness and structure in multiple directions from lung image. Brightness uniformity estimation uses $ELBP^{riu2}$. In order to extract texture features in multiple directions, we propose a modified extension of rotation invariant local binary pattern that uses a threshold value. At first LBP is introduced.

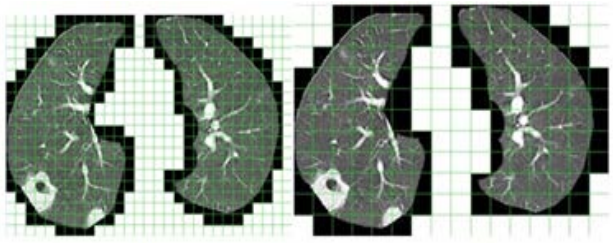

a b

Fig. 3 Different sub-regions. a) Small sub-regions; b) Large sub-regions

a. Local Binary Pattern (LBP)

The LBP [25] is a powerful tool for describing texture features and has been widely used in a large number of applications such as face recognition [31] and medical image analysis [32]. The first LBP operator, which was introduced by ojala et, al. in [25].

LBP is a simple method that generates binary codes by comparing points of the for example 3*3 neighboring pixels with respect to the center pixel value. It generates a binary code 0 if the value of neighbor pixel is smaller than that of the center pixel. Otherwise, it generates a binary code 1. Then the binary codes are multiplied with the corresponding weights and the results are summed up to generate an LBP code. This value is calculated as follow in Eq. (1):

$$LBP_{P,R}(x,y)=\sum_{i=0}^{P-1}s(g_i-g_c)2^i \quad (1)$$

$$s(g_i-g_c)=\begin{cases}1 & if\ \ g_i\geq g_c\\ 0 & else\end{cases} \quad (2)$$

where g_c is the pixel value of the center point and g_i is the pixel value of the neighboring pixel, P is the number of neighbor pixels, R is the radius.

Fig. 4 shows the process of generating LBP code. At last, each LBP code is used as a feature value. Also it can be used in a LBP histogram. Each bin of LBP histogram shows the number of a LBP code value. There are many versions of LBP that extract texture feature of image. Most of these methods are not rotate invariant. To obtain rotation invariant, the original LBP

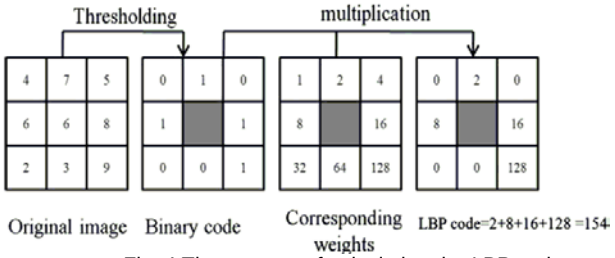

Fig. 4 The process of calculating the LBP code.

was then extended to a circular symmetric neighbor set of P members on a circular region with radius R using uniform patterns [26].The rotation invariance LBP (LBP^{riu2}) can be obtained as in Eq. (3).

$$LBP_{P,R}^{riu2}(x,y)=\begin{cases}\sum_{i=0}^{P-1}s(g_i-g_c) & if\ \ U(LBP_{P,R})\leq 2\\ P+1 & else\end{cases} \quad (3)$$

$$U(LBP_{P,R})=|\,s(g_{p-1}-g_c)-s(g_0-g_{c)}\,|+\sum_{i=1}^{P}|\,s(g_i-g_c)-s(g_{i-1}-g_{c)}\,| \quad (4)$$

Here, riu2 reflects that the rotation invariant uniform patterns have a U value of at most 2. U is used to estimate the uniformity that corresponds to the number of spatial transitions, i.e., bitwise 0/1 changes between successive bits in the circle. Fig.5 is an example of the local uniform pattern with different U. LBP^{riu2} is rotate invariant method and merges rotated features and produces only P+1 features rather that 2^p features of LBP.

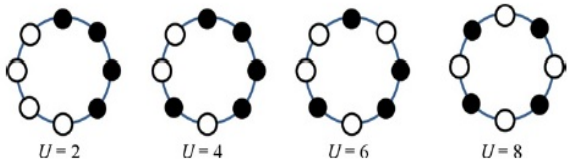

Fig. 5 An example of local binary patterns with different U.

LBP^{riu2} uses uniform local pattern by using U<=2. To further

$$ELBP_{P,R}^{riu4}(x,y)=\begin{cases}\sum_{i=0}^{P-1}|\,s(g_i-g_c)\,| & if\ \ U(ELBP_{P,R})\leq 4\\ P+1 & else\end{cases} \quad (6)$$

describe the brightness uniformity of the local patterns and make

$$s(g_i-g_c)=\begin{cases}1 & g_i>g_c\\ 0 & g_i=g_c\\ -1 & g_i<g_c\end{cases} \quad (5)$$

the LBP more distinctive, Uniformity Estimation Method (UEM)

[50] used $ELBP^{riu4}$ by redefining Eqs.(2)-(3) as Eqs.(5)-(6).

b) Proposed ELBP (TELBP)

As we can see from (5), the comparing result between the center point and its neighboring pixels is divided into three situations that are given by different labels (-1, 0, and 1). This new pattern can distinguish the brightness relationship between the center point and its neighboring pixels in more details. But it is more sensitive to noise rather than LBP. We proposed new method of ELBP which is named TELBP that uses threshold parameter T. This new method is more robust to noise and obtain information in multiple directions. So $TELBP^{riu2}$ is the same as $ELBP^{riu4}$ and only difference is shown in Eq.(7) instead of Eq.(5) and using U<=2 instead of U<=4. If CT images do not have noise, we must use T=0. If T=0, Eq.(7) is the same as Eq.(5). By setting T properly, the $TELBP^{riu2}$ is more robust to noise and produces better discrimination information than $ELBP^{riu4}$ and LBP^{riu2}. If R=1 in LBP^{riu2}, more than 90 percent of local pattern is uniform pattern. For R>1 this percentage decrease slightly (around 20 percent for R=2 and etc.). Therefore, it can be used to determine X value in (7). X must be set to 1 or 0 to produce uniform pattern. LBP^{riu2} uses uniform local binary pattern by using U<=2. So each undetermined bit in (7) Must set to 0 or 1 to produce uniform pattern. For example if 8 bits are 011X1000 so the X set to 1 to produce uniform pattern (U<=2) because 90 percent of pattern is uniform. If X set to 0 so U=4 and it is non uniform pattern. Also most of the patterns in texture are symmetric pattern. A pattern is symmetric if the number of 1 is equal or close to the number of 0 in transition bits of LBP. If more than one bit is undetermined. The undetermined bits set to 1 or 0 to produce uniform and symmetrical pattern. The pattern is symmetric if the number of 0 and 1 in transition bits is equal or close to each other. For example if transition bits are XX111100 it produces 4 combinations: 00111100, 11111100, 011111000 and 10111100. The last combination must remove because it is non uniform. The Second combination also removed because it is asymmetric. At last m=2 combinations 00111100 and 011111000 are remained. So 1/m is added to each histogram bin of these combinations or LBP codes. Each bin of histogram is used as a feature for classification. Using this proposed method increase the noise robustness of LBP. In our implementation value of T depends on the variance of noise in CT image (after preprocessing) the more variance of noise the greater value of T.

$$s(g_i - g_c) = \begin{cases} 1 & g_i - g_c > T \\ X & -T \le g_i - g_c \le T \\ 0 & g_i - g_c < -T \end{cases} \quad (7)$$

c. Texture Features Extraction

Now, for a point P (x, y), the $TELBP^{riu2}$ is employed to denote the brightness uniformity of the neighbors of P (x, y) and the gradient orientation difference that is applied to denote the local structural uniformity among P (x, y) and its neighbors. Suppose the number of neighboring points is P , defined radius is R, and neighboring points are $P(x_1, y_1),...,P(x_P, y_P)$ a pair of uniformity based values are defined between a given point P (x, y) and its neighbor point $P(x_n, y_n)$ based on Eq. (15). To describe the local structures, [50] proposed to apply the gradient orientations of the points.

$$M(TELBP^{riu2}, GOD \mid P, R) = \begin{bmatrix} F(0,0 \mid P,R) & F(0,1 \mid P,R) & \cdots & F(0,D \mid P,R) \\ F(1,0 \mid P,R) & F(1,1 \mid P,R) & \cdots & F(1,D \mid P,R) \\ \vdots & \vdots & \vdots & \vdots \\ F(L,0 \mid P,R) & F(L,1 \mid P,R) & \cdots & F(L,D \mid P,R) \end{bmatrix} \quad (11)$$

The gradient orientation is another good measure of representation of the image features [33,34]. If the image intensity function is shown as I (x, y). The gradient orientation of point P(x, y) is calculated as follows based on the Sobel mask as Eq.(8) and GOD (Gradient of Difference) is obtained as Eq. (9).

$$\theta(x,y) = \arctan\left(\frac{I(x,y+1) - I(x,y)}{I(x+1,y) - I(x,y)}\right) \quad (8)$$

$$GOD(x,y)_{x_n,y_n} = |\theta(x,y) - \theta(x_n,y_n)| \quad n = 1,..,P = 8 \quad (9)$$

Where g_c is the gray level of P (x, y). Similarly, the pairs of uniformity based values for P(x, y) and $P(x_1, y_1),...,P(x_8, y_8)$ (for P=8 neighbor points) can be obtained by Eq.(10). As we can see in Eq.(10), the $GTELBP^{riu2}$ is the gray level based $TELBP^{riu2}$, which is a combination of the gray level and the $TELBP^{riu2}$. The gray level is degraded by the $TELBP^{riu2}$. Thus, if the points around P(x, y) are uniform, $GTELBP^{riu2}$ will obtain a lower value or vice versa. Finally, the bright and structural uniformity can be estimated by applying Eq.(10).

$$GTELBP^{riu2}(x,y) = g_c * \frac{TELBP^{riu2}_{P,R}(x,y)}{P+1} \quad (10)$$

Now, a conditional probability density function F($GTELBP^{riu2}$;GOD|P,R) can be defined based on Eq.(11), where 0 ≤ $GTELBP^{riu2}$ ≤ L (suppose the gray level range is [0, L]), and 0≤GOD≤D (suppose the range of the degrees of gradient orientation difference is [0,D]). Finally, a co-occurrence matrix with the size of (L+1)*(D+1) can be used for making probability matrix as Eq.(11).

F (l, d| P, R) value is probably of gray scale l and gradient difference d in $GTELBP^{riu2}$ image. For each l value there are P values of d because of P neighbor points. So all of these P pair values must be applied to co-occurrence matrix.

Then some texture features are extracted from this matrix as Eqs.(12-18). In these seven features, entropy is an indication of the complexity within an image; a complex image produces a high entropy value [35]. Orientation difference is a measure of the image structure difference. If the local structures of an image are different from each other, Gradient Orientation difference is high and Gradient Orientation Uniformity is low. High Gray Level value and Homogeneity are two measures of the image brightness.

Entropy:

$$ENT = -\sum_{l=0}^{L}\sum_{d=0}^{D} F(l,d\,|P,R)\log(F(l,d\,|\,P,R)) \quad (12)$$

Gradient Orientation Uniformity (GOU):

$$GOU = \sum_{l=0}^{L}\sum_{d=0}^{D} F(l,d\,|P,R)\,Cos(d) \quad (13)$$

Gradient Orientation Difference (GOD):

$$GOD = \sum_{l=0}^{L}\sum_{d=0}^{D} F(l,d\,|P,R)\,Sin(d/2) \quad (14)$$

High Gray Level:

$$HGL = \sum_{l=0}^{L}\sum_{d=0}^{D} F(l,d\,|P,R)\,l^2 \quad (15)$$

Homogeneity:

$$HMG = \sum_{l=0}^{L}\sum_{d=0}^{D} \frac{F(l,d\,|\,P,R)}{1+l^2} \quad (16)$$

Moment:

$$MMT = \sum_{l=0}^{L}\sum_{d=0}^{D} \frac{F(l,d\,|\,P,R)^2}{1+l^2} \quad (17)$$

Energy:

$$ENG = \sum_{l=0}^{L}\sum_{d=0}^{D} F(l,d\,|\,P,R)^2 \quad (18)$$

If the image is bright, High Gray Level will achieve a high value and homogeneity obtains low value. The homogeneity is a measure of the structural uniformity of an image. It obtains a high value if the image is uniform, and vice versa. Also, Moment and Energy are two important features that are used to describe intensity of images. These 7 features are calculated for each sample (each sub-region of each segmented lung) and used by SVM for classification.

4 Experimental Result and Discussions

In this section, results of the proposed method are presented and compared with some high performance algorithms. In the experimental results, eight clinical data sets with 19 nodules approved by medical experts are used. There are 45 slices/scans among which four data sets are 5 mm thickness. Also, there are 11 solid and two non-solid nodules in these data sets. Here, we have seven lung wall attached, one bronchiole attached and five solitary nodules. Another four data sets include about 450 slices/scans. There are four solid and two cavity nodules in these images. Four of these nodules are lung wall attached, one of them is bronchiole attached and the other one is solitary. These data sets were obtained in TABA medical imaging center of Shiraz medical school. Also Some CT images of LIDC dataset are used in train and test part [36].

Lung segmentation method that is proposed in this paper based on concavity degree can be compared with some other lung segmentation methods. There are some lung segmentation methods based on rolling ball and morphological operation such as [13], [14] and [15] that are depend on radius of the ball and size of window but our proposed method is independent from this values. So, we propose a good method that extracted lung accurately that caused better results for the next steps. In the nodule detection, by using SVM classifier, the results of nodule detection have compared with some other methods. In this part by using TELBP instead of ELBP the accuracy of proposed method is increased and compared with three SGLDM, GLRLM, GLDM [16]. These three methods are not rotate invariant but our method is rotate invariant. Also our proposed method is compared with UEM [29]. UEM is a well-known and rotate invariant method. For feature extraction, image can divided into small or large such as Fig. 7 and for each sub-region texture features are extracted and used in co-occurrence matrix. LibSVM [37] classifier is used for train and test. 70% of images are used for train and 30% for test. We evaluated the performances of proposed method for nodule detection according to the Sensitivity, Specificity, and Accuracy that are related to True Positive, True Negative, False Positive, and False Negative as follows:

- True positive(TP): the number of abnormal sub-regions that are correctly classified.
- True negative (TN): the number of normal sub-regions that are correctly classified.
- False positive (FP): the number of normal sub-regions that are incorrectly classified as abnormal regions.
- False negative(FN): the number of abnormal sub-regions that are incorrectly classified as normal regions.

The Sensitivity, Specificity, and Accuracy are then defined as Eqs.(19-21).

$$Sensitivity = \frac{TP}{TP + FN} \quad (19)$$

$$Specificity = \frac{TN}{TN + FP} \quad (20)$$

$$Accuracy = \frac{TP}{TP + FN + TN + FP} \quad (21)$$

For a fair comparison, seven texture features for each method are extracted that we have mentioned before. The methods SGLDM, GLRLM, GLDM and UEM are used for comparing the results with proposed method. Texture features are extracted in four directions: 0, 45, 90, and 135 (for rotate variant methods). The inner distances for SGLDM and GLDM were set to 1; these provided the best result for all methods. For the proposed method, the best result was achieved by setting the number of neighboring pixels at 8 and setting the radius to 1. As these tables (TABLE 1 to 4) show, most of the time our proposed method reach to higher accuracy than other methods. These tables compare the accuracies of methods by using SVM classifier tool.

Considering the Table 1, it shows that proposed method has better accuracy rather than uniformity estimation method (UEM). The accuracy of proposed method outperforms the UEM method while the noise increases drastically. Both of proposed and UEM methods are rotation invariant. This table indicates the effects of noise correction method for different Gaussian noise values. Each Tables 2,3 and 4 determine the results of nodule detection, using GLDM,SGLDM and GLRLM and compare these results with proposed method. These three methods are not rotate invariant. Therefore in the CT images,

first we train SVM classifier by using original CT images, then in test part the rotated CT images are used and texture features are extracted by using rotated images in four directions: 0, 45, 90, and 135. Considering the result of Table 2, it shows that for all directions the GLDM has worse result than proposed method. Only for GLDM90 the specificity is the same as proposed method. Also the proposed method has better performance than SGLDM for all result values of Table 3. In this table only for SGLDM0 the sensitivity is better than proposed method. Table 4 show the result of nodule detection for proposed and GLRLM methods. It is simple to show that proposed method has better specificity in most cases but the sensitivity of it, is lower than that of GLRLM. It is because of the greater number of abnormal sub-regions that are incorrectly classified as normal regions in proposed method. Although the proposed method has lower sensitivity in some case, the overall accuracy of it is better than GLRLM in all cases. Furthermore, the proposed method is a rotation invariant method, however in these three methods the result of the process changes when the CT images are rotated. The results of these tables are related to the accuracy of nodule detection using large sub-regions for feature extraction and using in LibSVM. It is possible to use small or large sub-regions for train and test of SVM but using small sub-regions does not change these results significantly.

TABLE 1
COMPARING CLASSIFICATION ACCURACY OF UEM AND PROPOSED METHOD FOR IMAGES THAT INJECTED WITH GAUSSIAN NOISE (σ = 0, 0.03, 0.05,0.1).

Method	$\sigma = 0$	$\sigma = 0.03$	$\sigma = 0.05$	$\sigma = 0.1$
Proposed	98.00	96.60	93.80	91.40
UEM	97.20	93.80	90.20	86.20

TABLE 2
COMPARING CLASSIFICATION SENSITIVITY, SPECIFICITY AND ACCURACY OF GLDM AND PROPOSED METHOD IN FOUR DIRECTIONS (NO NOISE).

Method	Sensitivity(%)	Specificity(%)	Accuracy(%)
Proposed	96.40	99.60	98.00
GLDM 0	86.40	98.40	92.40
GLDM 45	92.00	98.50	95.25
GLDM 90	91.40	99.60	95.50
GLDM 135	93.20	98.20	95.70

TABLE 3
COMPARING CLASSIFICATION SENSITIVITY, SPECIFICITY AND ACCURACY OF SGLDM AND PROPOSED METHOD IN FOUR DIRECTIONS (NO NOISE).

Method	Sensitivity(%)	Specificity(%)	Accuracy(%)
Proposed	96.40	99.60	98.00
SGLDM 0	98.00	90.00	94.00
SGLDM 45	92.60	95.40	94.00
SGLDM 90	89.00	98.00	93.50
SGLDM 135	88.60	97.80	93.20

TABLE 4
COMPARING CLASSIFICATION SENSITIVITY, SPECIFICITY AND ACCURACY OF GLRLDM AND PROPOSED METHOD IN FOUR DIRECTIONS (NO NOISE)

Method	Sensitivity(%)	Specificity(%)	Accuracy(%)
Proposed	96.40	99.60	98.00
GLRLM 0	97.00	92.00	94.50
GLRLM 45	98.00	84.00	91.00
GLRLM 90	90.20	99.80	95.00
GLRLM 135	98.60	78.40	88.50

5 CONCLUSION

In this paper, an automatic method is proposed that detect lung nodule in CT images. The proposed method consists of three steps; 1) preprocessing and lung segmentation 2) feature extraction and 3) nodule detection (Classification) at the beginning of the process some enhancement methods are used to improve quality of image. Then a concavity degree method is used which can extract lung areas from the CT image. In this paper a version of local binary pattern is proposed to extract texture feature of nodules and using them for each sub-region of image. This method is robust to noise and correct noise effects by using uniform and symmetrical information of local patterns. Extracted features are used in a SVM classifier to detect sub-regions that contain nodule.

ACKNOWLEDGMENT

The author wishes to thank the Islamic Azad University, Fars Science and Research Branch for supporting this research.

REFERENCES

[1] T.K. Liang, T. Tanaka, H. Nakamura, A. Ishizaka, A neural network based computer-aided diagnosis of emphysema using CT lung images, in: Proceedings of the SICE Annual Conference, Kagawa University, Takamatsu City, Japan, September 1720,pp. 703709 (2007).

[2] B. Sahiner, H.-P.Chan, L.M.Hadjiiski, P.N. Cascade, E.A.Kazerooni, A.R.Chughtai, C. Poopat, T.Song, L.Frank, J.Stojanovska, A.Attili, Effect of CAD on Radiologists detection of lung nodules on thoracic CT scans : analysis of an observer performance study by nodule size, Acad. Radiol.y16(12)(2009).

[3] R.Yuan, P.M.Vos, P.L.Cooperberg, Computer-aided detection in screening CT for pulmonary nodules, Am.J.Roentgenol.186(5), (2006).

[4] K.Marten, C.Engelke, Computer-aided detection and automated CT volumetry of pulmonary nodules,Eur.Radiol.17(2007).

[5] Asem M. Ali, Ayman S. El-Baz, Aly A. Farag, A Novel framework for accurance lung segmentation using graph cuts, in Proc. of ISBI 2007, pp. 908 – 911.

[6] Nisar Ahmed Memon, Anwar Majid Mirza, and S.A.M. Gilani, "Deficiencies of Lung Segmentation Techniques using CT Scan Images for CAD", World Academy of Science, Engineering and Technology 2008

[7] M. Keshani, Z. Azimifar and R. Boostani, Lung Nodule Segmentation Using Active Contour Modeling ,6th Iranian Conference on Machine Vision and Image Processing, (2010).

[8] Zhang, X.; McLennan, G.; Hoffman, EA.; Sonka, M. Automated de-tection of small-size pulmonary nodules based on helical CT images; Proceedings of

19th International Conference on Information Pro cessing in Medical Imaging; Glenwood Springs (USA), (2005).

[9] S. Shimoyama, N. Homma, M. Sakai, T. Ishibashi, and M. Yoshizawa, Auto-detection of non-isolated pulmonary nodules connected to the chest walls in X-ray CT images, in Conf. IEEE ICCAS-SICE, (2009).

[10] H. Zhang, J.E. Fritts, S.A. Goldman, A fast texture feature extraction method for region-based image segmentation, Image and Video Communications and Processing , (2005).

[11] Z. Wang, A. Guerriero, M.D. Sario, Comparison of several approaches for the segmentation of texture images, Pattern Recognition Letters 17 (1996).

[12] Y. Zhang, X.J. He, J.H. Han, Texture feature-based image classification using wavelet package transform, Advances in Intelligent Computing 3644 (2005).

[13] R.W. Conners, C.A Harlow, A theoretical comparison of texture algorithms, IEEE Transactions: Pattern Analysis and Machine Intelligence (1980).

[14] T. Glatard, J. Montagnat, I.E. Magnin, Texture based medical image indexing and retrieval: application to cardiac imaging, in: Proceedings of the Sixth ACM SIGMM International Workshop on Multimedia Information Retrieval, New York, USA, October 1516, (2004).

[15] D.H. Kim, Image recommendation algorithm using feature-based collaborative lettering, IEICE TRANSACTIONS on Information and Systems E92-D , (2009).

[16] A.H. Mir, M. Hanmandlu, S.N. Tandon, Texture analysis of CT images, in: Engineering in Medicine and Biology Magazine, vol.14, IEEE, (1995).

[17] S.Ozekes, Rule based lung region segmentation and nodule detection via genetic algorithm rained template matching, IstanbulCom-mer.Univ.J.Sci.6 (11) (2007).

[18] S.Ozekes, O.Osman, O.N.Ucan, Nodule detection in a lung region that's segmented with using genetic cellular neural networks and 3D template matching with fuzzy rule based thresholding, KoreanJ.Radiol.9(2008).

[19] X.Ye, G.Beddoe, G.Slabaugh, Graph cut-based automatic segmentation of lung nodules using shape, intensity, and spatial features, in: The Second International Workshop on Pulmonary Image Analysis, pp.103113, (2009).

[20] M.Antonelli, G.Frosini, B.Lazzerini, F.Marcelloni, Automated detection of Pulmonary nodules in CT scans, in: International Conference on Computational Intelligence for Modeling, Control and Automation, vol.2,2005,pp.799803.

[21] A.E.-B.G.Gimelfarb, R.F.M.A.El-Ghar, Computer aided characterization of the solitary pulmonary nodule using volumetric and contrast enhancement features, Acad.Rodiol.1213101319, (2005).

[22] T.Messay, R.C.Hardie, S.K.Rogers, A new computationally efficient CAD system for pulmonary nodule detection in CT imagery, Med.ImageAnal.14 (3) 390406, (2010).

[23] M. Tan, R.Deklerck, B.Jansen, M.Bister, J.Cornelis, A novel computer-aided lung nodule detection system for CT images,Med.Phys.38(10)(2011).

[24] R. Opfer, R.Wiemker, Performance analysis for computer-aided lung nodule Detection on LIDC data, in: Proceedings of theSPIE,vol.6515, (2007).

[25] [25] T. Ojala, M. Pietikainen, D. Harwood, A comparative study of texture measures with classication based on feature distributions, Pattern Recognition (1996).

[26] T. Ojala, M. Pietikainen, T. Maenpaa, Multiresolution gray-scale and rotation invariant texture classification with local binary patterns, IEEE Transactions on Pattern Analysis and Machine Intelligence 24 (7) (2002).

[27] [27] R. C. Gonzalez, R. E. Woods, Digital Image Processing, Second Edition, Prentice hull (2002).

[28] Nobuyuki Otsu, A Threshold Selection Method From Gray Level Histogram, IEEE Transactions On System, Man And Cybernetics, Vol.9, PP. 62-67, (1979).

[29] S. Penga, D.Kim, S. Lee , M. Lim, "Texture feature extraction based on a uniformity estimation method for local brightness and structure in chest CT images", Computers in Biology and Medicine 40 ,931942, (2010).

[30] T.K. Liang, T. Tanaka, H. Nakamura, A. Ishizaka, A neural network based computer-aided diagnosis of emphysema using CT lung images, in: Proceedings of the SICE Annual Conference 2007, Kagawa University, Takamatsu City, Japan, September 1720, pp. 703709, (2007).

[31] T. Ahonen, A. Hadid and M. Pietikainen, Face description with local binary patterns: application to face recognition, in: Proceedings of the Eighth European Conference on Computer Vision, vol. 28, pp. 469481, (2004).

[32] G. Tian, H. Fu, D.D. Feng, Automatic medical image categorization and annotation using LBP and MPEG-7 Edge histograms, Proceedings of the Fifth International Conference on Information Technology and Application in Biomedicine, Shenzhen, China, pp. 5153,(2008).

[33] K. Mikolajczyk, C. Schmid, A performance evaluation of local descriptors, IEEE Transactions on Pattern Analysis and Machine Intelligence 27, 16151630, (2005).

[34] D.G. Lowe, Distinctive image features from scale-invariant key point, Computer Vision 2, (2004).

[35] B. Park, Y.R. Chen, Co-occurrence matrix texture features of multi-spectral images on poultry carcasses, Journal of Agricultural Engineering Research Volume 78 (2) 127139, (2001).

[36] https://wiki.cancerimagingarchive.net/display/Public/LIDC-IDRI

[37] www.csie.ntu.edu.tw/cjlin/libSvm.

IJSER